

The typical mass ratio and typical final spin in supermassive black hole mergers

László Á. Gergely^{1,2†}, Peter L. Biermann^{3,4,5,6,7‡}

¹ Department of Theoretical Physics, University of Szeged, Hungary

² Department of Experimental Physics, University of Szeged, Hungary

³ Max-Planck-Institut für Radioastronomie, Auf dem Hügel 69, Bonn, Germany

⁴ FZ Karlsruhe and Physics Department, University of Karlsruhe, Germany

⁵ Department of Physics and Astronomy, University of Alabama, Tuscaloosa, AL, USA

⁶ Department of Physics, University of Alabama at Huntsville, AL, USA

⁷ Department of Physics and Astronomy, University of Bonn, Germany

† E-mail: gergely@physx.u-szeged.hu ‡ E-mail: plbiermann@mpifr-bonn.mpg.de

We prove that merging supermassive black holes (SMBHs) typically have neither equal masses, nor is their mass ratio too extreme. The majority of such mergers fall into the mass ratio range of 1 : 30 to 1 : 3, implying a spin flip during the inspiral. We also present a simple expression for the final spin χ_f of the emerging SMBH, as function of the mass ratio, initial spin magnitudes, and orientation of the spins with respect to the orbital plane and each other. This formula approximates well more cumbersome expressions obtained from the fit with numerical simulations. By integrating over all equally likely orientations for precessing mergers we determine a lower approximant to the final spin distribution as function of the mass ratio alone. By folding this with the derived mass ratio dependent merger rate we derive a *lower* bound to the typical final spin value after mergers. We repeat the procedure deriving an *upper* bound for the typical spin in the case when the spins are aligned to the orbital angular momentum, such that there is no precession in the system. Both slopes of χ_f as function of the initial spins being smaller than one lead to two attractors at $\chi_f^{prec} = 0.2$ and $\chi_f^{align} = 0.45$, respectively. Real mergers, biased toward partial alignment by interactions with the environment (accretion, host galaxy, etc.) would generate a typical final spin lying between these two limiting values. These are the typical values of the spin after the merger, starting from which the spin can built up by further gaseous accretion.

PACS numbers:

I. INTRODUCTION

Einstein's general theory of relativity predicts that the coalescence of two compact objects (neutron stars or black holes) is accompanied (and driven by) intense gravitational radiation. Stellar mass (a few to a few ten solar masses, M_\odot) black hole binaries emit gravitational waves with frequency falling into the best sensitivity range of LIGO [1], Virgo [2] and GEO600 [3] Earth-based interferometric gravitational wave detectors. Up to date there are very few observations [5] indicating the existence of intermediate mass black holes. Binaries formed by such black holes would emit gravitational waves falling into the frequency range of third generation gravitational wave detectors, like the Einstein Telescope [4].

Supermassive black holes (SMBHs) with masses of $10^6 \div 3 \times 10^9 M_\odot$ (or perhaps even higher) on the other hand are quite frequent, residing in the centre of each sufficiently massive galaxy. Their growth occurs by accretion phases and by mergers, the estimated contribution of each of these processes to the growth of mass being model-dependent. Recent observations [6] show that some galaxies never merge, and yet may have central black holes; representing either the pure SMBH birth population, or the birth population with some gaseous accretion.

The accretion process has been modeled with the inclusion of magnetic fields, electromagnetic radiation of

the disk and energetic jets transporting angular momentum from the polar regions [7]-[9]. Beside increasing the mass, accretion will also spin up the black holes. The spin limit reached due to accretion by canonical black holes (the system of a black hole and electromagnetically radiating accretion disk), as expressed in terms of the dimensionless spin is $\chi_{can} = 0.998$, close to the theoretically allowed maximum for a black hole, the unity. Indeed, such a high spin powering the jets seems compulsory for understanding the low energy cutoff in the energetic electron spectra of jets in radio galaxies [10]. Active Galactic Nuclei, in particular the closest, Cen A are the most likely sources of for the Ultra High Energy Cosmic Rays [11].

When galaxies merge, eventually their central SMBHs will also do so. Dynamical friction transfers some of the orbital angular momentum of the binary black hole system to the stellar environment, being ejected at the poles, a process which drives the system through the last parsec [12]. Other mechanisms to overcome the last parsec are relaxation processes due to cloud/star – star interactions, repopulating the stellar orbits in the center of the galaxy [13], binary orbital decay by three-body interactions in the gravitationally bound stellar cusps [14], or the interplay of three accretion disks: one around each black hole and the third, circumbinary, removing orbital angular momentum from the binary [15].

At about 0.005 parsecs gravitational radiation takes over dynamical friction as the leading dissipative effect

[16]. For many SMBH binaries the gravitational waves emitted in the process of coalescence fall into the frequency range the long-delayed space mission LISA [17]. Depending on how rich in gas the binary environment may be and whether there any circumbinary disk has been formed, certain alignment between the proper spins and the orbital angular momentum could occur due to the Bardeen-Petterson effect (based in turn on the Lense-Thirring precession) [18]. The two situations which could occur are the mergers precessing under random angle (also known as dry mergers) and non-precessing mergers, implying complete alignment of the spins and orbital angular momentum (wet mergers). The randomness in the orientation of precessing mergers typically reduces the final spin [19]. For equal mass precessing mergers this varies from 0.69 for non-spinning black holes up to values of 0.73 for maximally spinning black holes [20]. For a mass ratio 1 : 10 the range of final spins opens up to the interval between 0.2 and 0.83, respectively, as function of the initial spins. For non-precessing mergers all configurations would practically conserve a high initial spin during the inspiral.

When the two black holes are at large distances, the orbital angular momentum L is always much larger than the individual spins S_i . However at the characteristic radius $r^* \approx 0.005$ parsec¹ (and the corresponding post-Newtonian (PN) parameter $\varepsilon^* = Gm/c^2 r^* \approx 10^{-3}$, defining the beginning of the inspiral, see [16]), where gravitational radiation takes over dynamical friction as the leading order dissipative effect, the ratios $S_i/L \approx (\varepsilon^*)^{1/2} q^{3-2i} \chi_i$ depend on the mass ratio $q \geq 1$. For a maximally spinning larger black hole and separation r_* the ratio is one at about $q \approx 30$. For mass ratios larger than 30 therefore the spin dominates over the orbital angular momentum during the whole inspiral.

During the inspiral gravitational radiation further reduces the orbital angular momentum, but not the spin magnitudes. The spins will only precess driven by the leading order spin-orbit coupling and corrections due to spin-spin and mass quadrupole - mass monopole coupling [32]. In the process the direction of the total angular momentum remains unchanged, in an averaged sense over one radial orbit [33].

Gravitational radiation does not modify this conclusion on short time-scales. Radiative evolutions with spin-orbit [34], spin-spin [35] and mass quadrupole - mass monopole [36] couplings have been investigated, and their analysis in Ref. [37] lead to the important result that the instantaneous radiative changes of the spins average out during a radial period. On this timescale therefore there

is no secular radiative change of the spin vectors at all:

$$\left\langle \frac{d\mathbf{S}_i}{dt} \right\rangle = 0. \quad (1)$$

This result confirms that the spin dynamics can be regarded as a pure precession, up to high PN orders including radiation reaction, on the timescales comparable with a radial orbit. On much larger timescales however the spin vector will undergo a reorientation (spin-flip), as explained in detail in Ref. [16].

There are several scenarios possible, according to the actual mass ratio:

a) The masses are comparable $m_2 \approx m_1$. In this case at the end of the inspiral (when the PN approximation breaks down) the orbital angular momentum still dominates over the spins [16], [21]. Radiating away this remnant orbital angular momentum during the merger phase, while extrapolating the conservation of the direction of the total angular momentum and of the individual spin magnitudes to this phase [38], [39] could significantly reduce the final spin in all cases when the individual spins were severely misaligned with each other and with the orbital angular momentum. Such a misalignment would be typical in the case of precessing mergers. Therefore for equal masses in a precessing merger a not too high final spin can be considered typical.

b) The mass ratio is in the range 1 : 30 to 1 : 3. In this case the orbital angular momentum dominates over the spin only at the beginning of the inspiral, and as such is roughly aligned with the total angular momentum. At the end of the inspiral however the orbital angular momentum becomes smaller than the dominant spin, which has therefore to be reoriented towards the invariant total angular momentum direction. For precessing mergers this process causes a spin-flip during the inspiral, but does not reduce significantly the magnitude of the dominant spin [16], [21]. Non-precessing mergers on the other hand already imply an alignment of the spins and orbital angular momentum, therefore neither the spin magnitude, nor its direction will be changed by this process. In both cases, whatever happens to the orbital angular momentum during the plunge, its small value (compared to the dominant spin) at the end of the inspiral will obstruct any serious further change in the final spin.

In this mass ratio range therefore the magnitude of the dominant spin will not be much reduced by the merger, nevertheless a significant reorientation of its direction during the inspiral will typically occur for precessing mergers, which could be followed only by a minor further spin-flip during the plunge.

c) The mass ratio is less than 1 : 30. Then the orbital angular momentum is too small from the beginning of the inspiral to modify the dominant spin. Neither its magnitude, nor its direction are affected and we practically face the inspiral of a test mass into the much larger black hole.

In this paper we revisit the merger process, based on the recent data of Ref. [22]. We first derive the SMBH

¹ The distance r^* depends weakly, as $m^{5/11}$ on the total mass and negligibly, as $\eta^{2/11}$ on the symmetric mass ratio $\eta = \mu/m = (q^{1/2} + q^{-1/2})^{-2}$, where $\mu = m_1 m_2 / m$ is the reduced mass.

mass distribution. In Section II we fit a broken power law for the differential mass function, then, based on this fit and a number of simple and reasonable assumptions we derive the mass ratio distribution. We note that the results of Ref. [22] are fully consistent with earlier results based on much smaller statistics [40].

Next we derive in Section III a simple approximant for the final spin of the emerging SMBH, as function of the mass ratio, initial spin magnitudes, and orientation of the spins with respect to the orbital plane. In the Appendix we compare the approximant with the more cumbersome expressions existing in the literature, which were obtained by fit to numerical simulations.

In Subsection IV A we adopt the configuration of precessing mergers, which allow for all relative spin and orbital angular momentum orientations on equal footing, lowering the chances for a large final spin after the merger. By integrating over all orientations in the precessing merger limit (without allowing any preference for alignment), for any initial spin set we determine a lower approximant to the final spin distribution as function of the mass ratio alone. By folding this with the previously derived mass ratio dependent merger rate, we obtain a *lower bound to the typical final spin* after SMBH mergers.

By contrast, in the non-precessing merger limit there is a perfect alignment of the spins with the orbital angular momentum, hence the integration should be carried on for this configuration alone, and only over the mass ratios, folded with the mass ratio distribution. By this method, in Subsection IV B we get an *upper bound for the typical final spin*.

We discuss the implications of our results and present the concluding remarks in Section V.

II. MASS RATIOS IN SMBH MERGERS

In Ref. [16] we gave a simple preliminary estimate of the typical mass ratio of merging SMBHs. We revisit the problem more rigorously here, both from a mathematical point of view and by employing new, more precise data on SMBH masses, presented in Ref. [22]. We do note that selection effects strongly influence some statistical arguments, in the case, that selection is based on detectable activity at the center of a galaxy for instance, on a far-infrared or ultra-violet excess; in the first case this could be due to selecting for central emission lines, in the second due to a central star-burst, and in the third to a visible central accretion disk. Our approach, taken in this paper, does suffer from the selection effect, that the work done by [22] used the colors of an old stellar population as the starting point, and then cut the sample to include only early Hubble type galaxies. However, allowing for a sample of late Hubble type galaxies would not increase the merger rate very much, since such galaxies usually suffer few if any mergers [6].

A. The differential mass function

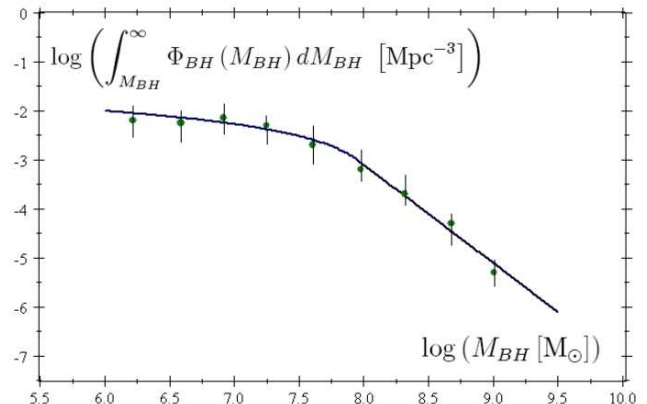


FIG. 1: (Color online) The integral mass function represented on logarithmic scale shows a remarkably good fit to the data from Ref. [22]. The differential mass function is taken as a broken power law with powers -1 and -3 , the breakpoint being at $8.9 \times 10^7 M_{\odot}$.

The SMBH distribution $\Phi_{BH}(M_{BH})$ can be interpreted as a power law with an exponential cutoff [22]. This can be well approximated by a broken power law [23]-[25], also confirmed by the survey [26]. The SMBH integral mass function data represented on Fig 5. of Ref. [22], after omitting the first two data points which do not refer to black holes, but rather to nuclear star clusters [27], also suggest the differential mass function $\Phi_{BH}(M_{BH}) \propto M_{BH}^{-\tilde{\alpha}}$, with $\tilde{\alpha} = 1$, starting from the lower mass limit of $m_a \approx 10^6 M_{\odot}$ to the breakpoint, which is approximately at $m_* \approx 10^8 M_{\odot}$; then $\Phi_{BH}(M_{BH}) \propto M_{BH}^{-\tilde{\beta}}$, with $\tilde{\beta} = 3$, starting from m_* to the upper mass limit, taken here as $m_b \approx 3 \times 10^9 M_{\odot}$. We prove this statement in the remaining part of the subsection.²

The SMBH data is represented on Fig 1, which shows the integral mass function $\int_{M_{BH}}^{\infty} \Phi(M_{BH}) dM_{BH}$ (in Mpc^{-3}) as a function of the SMBH masses (in M_{\odot}), represented on log-log scale. Due to the breakpoint (and by normalizing all masses to m_*), the integral mass function

² Note, that the lower mass data points were not important for the considerations in Ref. [22], concerned mainly with the highest energy cosmic rays, such that a different fit of $\tilde{\alpha}_{CB} = 2$ was advanced there. Nevertheless the supermassive black holes with lower mass are important in the merger statistics, therefore in this paper we chose $\tilde{\alpha} = 1$ due to the tendency of the first data points to be aligned horizontally (see Fig 1). The limit m_a is lowered here as compared to the choice of Ref. [16] such that the mass of the SMBH in the centre of our Galaxy is not the lower mass limit any more.

for any $M_{BH} \leq m_*$ is

$$\begin{aligned}
& \int_{M_{BH} \leq m_*}^{\infty} \Phi(M_{BH}) dM_{BH} \\
&= k \int_{M_{BH}}^{m_*} \left(\frac{M_{BH}}{m_*}\right)^{-1} dM_{BH} \\
&\quad + k \int_{m_*}^{\infty} \left(\frac{M_{BH}}{m_*}\right)^{-3} dM_{BH} \\
&= km_* \ln \left(\frac{M_{BH}}{m_*}\right) \Big|_{M_{BH}}^{m_*} - \frac{1}{2} km_* \left(\frac{M_{BH}}{m_*}\right)^{-2} \Big|_{m_*}^{\infty} \\
&= km_* \left[\frac{1}{2} - \ln \left(\frac{M_{BH}}{m_*}\right) \right], \tag{2}
\end{aligned}$$

while for any $M_{BH} \geq m_*$ is, respectively

$$\begin{aligned}
& \int_{M_{BH} \geq m_*}^{\infty} \Phi(M_{BH}) dM_{BH} \\
&= k \int_{M_{BH}}^{\infty} \left(\frac{M_{BH}}{m_*}\right)^{-3} dM_{BH} \\
&= -\frac{1}{2} km_* \left(\frac{M_{BH}}{m_*}\right)^{-2} \Big|_{M_{BH}}^{\infty} = \frac{1}{2} km_* \left(\frac{M_{BH}}{m_*}\right)^{-2} \tag{3}
\end{aligned}$$

Here k is a dimensional normalization constant. Both expressions reduce to $km_*/2$ at $M_{BH} = m_*$. Comparing with the data at m_* allows to fix $\log(km_*/2) \approx -3$, thus $km_*/2 = 10^{-3}$. Therefore

$$\begin{aligned}
& \log \int_{M_{BH}}^{\infty} \Phi(M_{BH}) dM_{BH} = -3 \\
& + \log \left(\begin{array}{l} 1 + 4.6(\log m_* - x), \text{ if } M_{BH} \leq m_* \\ 10^{-2x} m_*^2, \text{ if } M_{BH} \geq m_* \end{array} \right) \tag{4}
\end{aligned}$$

where $x = \log M_{BH}$. Because M_{BH} is given in solar masses, so is m_* . The broken power law with powers -1 and -3 gives the best fit with the data by setting the breakpoint at $m_* = 10^{7.95} M_{\odot} \approx 8.9 \times 10^7 M_{\odot}$, as seen on Fig 1. (Note that the breakpoint turns out to be shifted as compared with the number given in Ref. [16].) The fit is remarkable, the sum of the squares of the deviances between the points and the function values, divided by the square of the error bars is only 0.22.

B. SMBH mass ratio distribution

Based on the new SMBH mass function derived in the previous subsection here we work out the estimates for the likelihood of the mass ratios, following the logic of Ref. [16]. However the changed mass values imply more cases to be included in the analysis.

The number of encounters for a given mass ratio $q = m_1/m_2 \geq 1$, represented as $d\mathcal{N}/dq$ is proportional to the product of the distribution functions for both black holes,

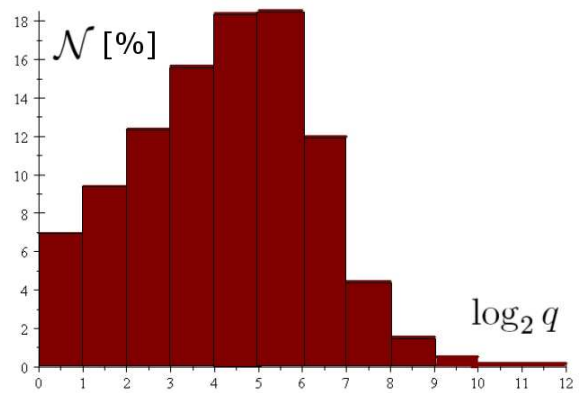


FIG. 2: (Color online) The number of SMBH encounters with mass ratios q as function of $\log_2 q$.

folded with the merger probability F and integrated over the mass m_2 of the smaller black hole:

$$\frac{d\mathcal{N}(q)}{dq} \propto \int_{m_a}^{m_b/q} \Phi_{BH}(m_2) \Phi_{BH}(qm_2) F(q, m_2) dm_2. \tag{5}$$

The merger probability in turn is proportional to the cross section (we neglect the weak dependence on the relative velocity of galaxies as these are not too high, the Universe being not old enough for mass segregation).

In order to determine the cross section, we assume that each galaxy merger is followed by the merger of their central SMBHs. Therefore we basically evaluate the cross section of merging galaxies. Further, we note that the masses of the galaxies and their central SMBHs correlate due to

- the correlation of the mass of the central SMBH with the mass of the host galactic bulge [28],
- the proportionality of the mass of the central SMBH with both the spheroidal galaxy mass component and the total mass (including dark matter) of the galaxy [29].

It is likely that the more massive SMBH, thus the most massive galaxy dominates the cross section, thus the merger rate F . As the cross section is a function of the galaxy mass (thus SMBH mass), we take $F \sim (qm_2)^\xi$. We chose $\xi = 1/2$ based on the following observation:

- the comparison of our galaxy with dwarf spheroidals shows that an increase by a factor of 10 in radius (thus 10^2 in cross section) is accompanied by an increase by a factor of 10^4 in mass [30]-[31].

The break point m_* splits the SMBH range into two intervals, encompassing a mass range of about a factor of $q_1 = 89$ and $q_2 = 36$. Thus (by normalizing all masses

to m_*) we estimate for any $q \in [1, 36]$ the number of encounters as

$$\begin{aligned} \frac{d\mathcal{N}(q)}{dq} \Big|_{q \in [1, 36]} &\propto \int_{m_a}^{m_*/q} \left(\frac{m_2}{m_*}\right)^{-\tilde{\alpha}} \left(\frac{m_2 q}{m_*}\right)^{-\tilde{\alpha}} \left(\frac{m_2 q}{m_*}\right)^\xi dm_2 \\ &+ \int_{m_*/q}^{m_*} \left(\frac{m_2}{m_*}\right)^{-\tilde{\alpha}} \left(\frac{m_2 q}{m_*}\right)^{-\tilde{\beta}} \left(\frac{m_2 q}{m_*}\right)^\xi dm_2 \\ &+ \int_{m_*}^{m_b/q} \left(\frac{m_2}{m_*}\right)^{-\tilde{\beta}} \left(\frac{m_2 q}{m_*}\right)^{-\tilde{\beta}} \left(\frac{m_2 q}{m_*}\right)^\xi dm_2. \end{aligned} \quad (6)$$

The first, second and third lines of the right hand side of Eq. (6) contain, respectively, the mergers of: two SMBHs from the lower mass interval; one SMBH from the lower, the other from the higher mass interval; and both SMBHs from the upper mass interval. The condition $q \leq q_2$ assures that the upper limit of the integrals is larger than the lower limit.

For $q \in [36, 89]$ there are two contributions, arising from the combination of either two light or a light and a heavy SMBHs:

$$\begin{aligned} \frac{d\mathcal{N}(q)}{dq} \Big|_{q \in [36, 89]} &\propto \int_{m_a}^{m_*/q} \left(\frac{m_2}{m_*}\right)^{-\tilde{\alpha}} \left(\frac{m_2 q}{m_*}\right)^{-\tilde{\alpha}} \left(\frac{m_2 q}{m_*}\right)^\xi dm_2 \\ &+ \int_{m_*/q}^{m_b/q} \left(\frac{m_2}{m_*}\right)^{-\tilde{\alpha}} \left(\frac{m_2 q}{m_*}\right)^{-\tilde{\beta}} \left(\frac{m_2 q}{m_*}\right)^\xi dm_2. \end{aligned} \quad (7)$$

The condition $q \leq q_1$ again assures that the upper limit of the integrals is larger than the lower limit.

Finally for $q \in [89, 3000]$ there is one single contribution

$$\frac{d\mathcal{N}(q)}{dq} \Big|_{q \in [89, 3000]} \propto \int_{m_a}^{m_b/q} \left(\frac{m_2}{m_*}\right)^{-\tilde{\alpha}} \left(\frac{m_2 q}{m_*}\right)^{-\tilde{\beta}} \left(\frac{m_2 q}{m_*}\right)^\xi dm_2. \quad (8)$$

Eq. (7) expresses the encounters of a light SMBH from the lower interval with a heavy SMBH from the upper interval.

Integration over m_2 gives

$$\begin{aligned} \frac{d\mathcal{N}(q)}{dq} \Big|_{q \in [1, 36]} &\propto \frac{q^{-1+\tilde{\alpha}} - q_1^{-1-\xi+2\tilde{\alpha}} q^{\xi-\tilde{\alpha}}}{1 + \xi - 2\tilde{\alpha}} \\ &+ \frac{q^{\xi-\tilde{\beta}} - q^{-1+\tilde{\alpha}}}{1 + \xi - \tilde{\alpha} - \tilde{\beta}} + \frac{q_2^{1+\xi-2\tilde{\beta}} q^{-1+\tilde{\beta}} - q^{\xi-\tilde{\beta}}}{1 + \xi - 2\tilde{\beta}}, \end{aligned} \quad (9)$$

$$\begin{aligned} \frac{d\mathcal{N}(q)}{dq} \Big|_{q \in [36, 89]} &\propto \frac{q^{-1+\tilde{\alpha}} - q_1^{-1-\xi+2\tilde{\alpha}} q^{\xi-\tilde{\alpha}}}{1 + \xi - 2\tilde{\alpha}} \\ &+ \frac{\left(q_2^{1+\xi-\tilde{\alpha}-\tilde{\beta}} - 1\right) q^{-1+\tilde{\alpha}}}{1 + \xi - \tilde{\alpha} - \tilde{\beta}}. \end{aligned} \quad (10)$$

and

$$\frac{d\mathcal{N}(q)}{dq} \Big|_{q \in [89, 3000]} \propto \frac{q_2^{1+\xi-\tilde{\alpha}-\tilde{\beta}} q^{-1+\tilde{\alpha}} - q_1^{-1-\xi+\tilde{\alpha}+\tilde{\beta}} q^{\xi-\tilde{\beta}}}{1 + \xi - \tilde{\alpha} - \tilde{\beta}}. \quad (11)$$

(We have employed $m_b/m_* = q_2$ and $m_*/m_a = q_1$.) With the preferred parameter values $\tilde{\alpha} = 1$, $\tilde{\beta} = 3$ and $\xi = 1/2$, $q_1 = 89$, $q_2 = 36$ the number of encounters for the three ranges simplifies to

$$\begin{aligned} \frac{d\mathcal{N}(q)}{dq} \Big|_{q \in [1, 36]} &= \frac{9.3964 \times 10^{-2}}{q^{0.5}} - \frac{8.8536 \times 10^{-4}}{q^{2.5}} \\ &- 1.0982 \times 10^{-10} q^2 - 7.9681 \times 10^{-3}, \\ \frac{d\mathcal{N}(q)}{dq} \Big|_{q \in [36, 89]} &= \frac{9.3964 \times 10^{-2}}{q^{0.5}} - 7.9686 \times 10^{-3} \\ \frac{d\mathcal{N}(q)}{dq} \Big|_{q \in [89, 3000]} &= \frac{148.86}{q^{2.5}} - 2.5618 \times 10^{-7} \end{aligned} \quad (12)$$

Here we have normalized such that

$$\begin{aligned} \int_1^{36} \frac{d\mathcal{N}(q)}{dq} \Big|_{q \in [1, 36]} dq + \int_{36}^{89} \frac{d\mathcal{N}(q)}{dq} \Big|_{q \in [36, 89]} dq \\ + \int_{89}^{3000} \frac{d\mathcal{N}(q)}{dq} \Big|_{q \in [89, 3000]} dq = 1 \end{aligned} \quad (13)$$

holds.

Defining the number of encounters in a mass ratio interval $[q_1, q_2]$ as $\mathcal{N}_{q_1 \div q_2} = \int_{q_1}^{q_2} \frac{d\mathcal{N}(q)}{dq} dq$ we obtain the percentages of the mergers with the mass ratio ranges falling between $[1, 3]$, $[3, 30]$, $[30, 100]$ and $[100, 3000]$, respectively as

$$\begin{aligned} \mathcal{N}_{1 \div 3} &= 12.1 \% , \quad \mathcal{N}_{3 \div 30} = 48.9 \% , \\ \mathcal{N}_{30 \div 100} &= 29.2 \% , \quad \mathcal{N}_{100 \div 3000} = 9.8 \% . \end{aligned} \quad (14)$$

The distribution of the mass ratios is shown in more detail on the histogram of Fig 2.

The most likely mass ratio range, occurring in approximately half of the mergers, turns out to be $q \in (3, 30)$, in agreement with the rough estimate of Ref. [16]. This is the mass ratio, where a spin flip occurs during the inspiral [16]. The second most numerous mass ratio range, approximately in 30% of the cases is for $q \in (30, 100)$. Both the comparable mass case with $q \in (1, 3)$ and the extremal mass ratio case, defined here as $q \in (100, 3000)$ represent just about 10% each of the SMBH mergers. This important result makes compulsory to model SMBH mergers for non-equal masses.

III. AN APPROXIMATE FINAL SPIN FORMULA IN SMBH MERGERS

In this section we propose a formula for the final spin, which on the one hand approximates reasonably well

more cumbersome expressions derived from fits with numerical runs, on the other hand is simple enough to facilitate the numerical integrations we will carry on in the remaining part of the paper. In this section we use $\nu = q^{-1}$.

In the system with the Newtonian orbital angular momentum on the z -axis and the periastron on the x -axis the spins are

$$\mathbf{S}_i = \frac{G}{c} m \mu \nu^{2i-3} \chi_i (\sin \kappa_i \cos \zeta_i, \sin \kappa_i \sin \zeta_i, \cos \kappa_i) .$$

The magnitude of the total spin $\mathbf{S} = \mathbf{S}_1 + \mathbf{S}_2$ is found from

$$\begin{aligned} \mathbf{S}^2 &= [\mathbf{S}_1^2 + 2\mathbf{S}_1 \cdot \mathbf{S}_2 + \mathbf{S}_2^2]^{1/2} \\ &= \frac{G}{c} m \mu \left[\sum_{i=1,2} (\nu^{2i-3} \chi_i)^2 + 2\chi_1 \chi_2 \cos \gamma \right]^{1/2} \end{aligned}$$

with

$$\cos \gamma = \cos \kappa_1 \cos \kappa_2 + \sin \kappa_1 \sin \kappa_2 \cos (\zeta_2 - \zeta_1) \quad (15)$$

while the orbital angular momentum (assuming circular orbits, thus $L_N = \mu r v$), to leading order can be written as

$$\mathbf{L}_N = \frac{G}{c} m \mu \varepsilon^{-1/2} (0, 0, 1) ,$$

where $\varepsilon = Gm/c^2 r = v^2/c^2$ is the post-Newtonian parameter. (This parameter increases as the black holes approach each other.)

The dimensionless version $\mathfrak{J} = cJ/Gm\mu$ of the magnitude of the total angular momentum reads

$$\begin{aligned} \mathfrak{J} &= \frac{c}{Gm\mu} [(\mathbf{L}_N + \mathbf{S}) \cdot (\mathbf{L}_N + \mathbf{S})]^{1/2} \\ &= [\mathbf{L}_N^2 + 2\mathbf{L}_N \cdot (\mathbf{S}_1 + \mathbf{S}_2) + \mathbf{S}^2]^{1/2} \\ &= [\varepsilon^{-1} + 2\varepsilon^{-1/2} \sum_{i=1,2} \nu^{2i-3} \chi_i \cos \kappa_i \\ &\quad + \sum_{i=1,2} (\nu^{2i-3} \chi_i)^2 + 2\chi_1 \chi_2 \cos \gamma]^{1/2} . \end{aligned}$$

The final spin magnitude is denoted

$$S_f = \frac{G}{c} m_f^2 \chi_f .$$

We identify as an upper limit for the final spin the magnitude of the total angular momentum at the end of the inspiral, obtaining $\chi_f = \eta (m/m_f)^2 \mathfrak{J}_f$. Here $\mathfrak{J}_f = \mathfrak{J}(\varepsilon = \varepsilon_f)$ and $\eta = \mu/m = \nu(1+\nu)^{-2}$. By introducing the efficiency of mass conversion into gravitational radiation as $\epsilon_{GW} = 1 - m_f/m$, we can express $m/m_f = (1 - \epsilon_{GW})^{-1}$. Hence

$$\begin{aligned} \chi_f &= \frac{\eta}{(1 - \epsilon_{GW})^2} [\varepsilon_f^{-1} + 2\varepsilon_f^{-1/2} \sum_{i=1,2} \nu^{2i-3} \chi_i \cos \kappa_i \\ &\quad + \sum_{i=1,2} (\nu^{2i-3} \chi_i)^2 + 2\chi_1 \chi_2 \cos \gamma]^{1/2} \quad (16) \end{aligned}$$

We are interested in establishing a lower boundary for the value of the final spin, thus we set the efficiency to zero. The maximal value of the bracket for any given χ_i arises when the spins are aligned with the orbital angular momentum:

$$\chi_f^{\max} = \eta \mathfrak{J}_f^{\max} = \eta (\varepsilon_f^{-1/2} + \nu^{-1} \chi_1 + \nu \chi_2) \quad (17)$$

With $\varepsilon_f^{-1/2} = 2$ (at two Schwarzschild radii, this is the radius of the innermost bound circular orbit in the Schwarzschild geometry) and for maximal spins this gives $\chi_f^{\max} = 1$, irrespective of the actual value of ν . Therefore we normalize χ_f by setting $\varepsilon_f^{-1/2} = 2$ in Eq. (16), and obtain a very simple expression for the final spin:

$$\begin{aligned} \chi_f &= \frac{\nu}{(1+\nu)^2} [4 + 4 \sum_{i=1,2} \nu^{2i-3} \chi_i \cos \kappa_i \\ &\quad + \sum_{i=1,2} (\nu^{2i-3} \chi_i)^2 + 2\chi_1 \chi_2 \cos \gamma]^{1/2} . \quad (18) \end{aligned}$$

When the mass ratio is extreme ($\nu \rightarrow 0$), Eq. (18) correctly reproduces $\chi_f = \chi_1$, a result to be expected from the test particle limit. This final spin function qualitatively reproduces well the more cumbersome final spin expressions found in the literature from fits with numerical runs. In the Appendix we compare in detail the expression (18) with the one presented in Ref. [39], finding that for the largest part of the parameter space it slightly underestimates the final spin.

IV. THE TYPICAL FINAL SPIN

A. Precessing (randomly oriented) mergers

In this subsection we discuss the typical spin in the merger of two black holes by assuming generic precessing mergers. As this implies complete randomness in the relative angular momenta orientations, we integrate the final spin formula (18) over all possible orientations. Then we weight this orientation independent, but still mass ratio dependent final spin with the probabilities for a given mass ratio (12) derived earlier in Section II and integrate over the mass ratios, obtaining a typical final spin as function of initial spin magnitudes only. As the integration over the mass ratio implies to integrate over q (according to the method of evaluating the merger rate), we will rewrite $\nu = q^{-1}$ in all expressions.

1. Mass ratio dependent typical final spin

We first integrate the expression of the final spin (18) over all spin directions. By adopting the precessing merger model, we allow for random spin orientations. The assumption of randomness sets $\cos \kappa_i$ and ζ_i , the cosine of the spin polar angles and the spin azimuthal angles

as evenly distributed random variables. Instead of the individual azimuthal angles, the combination $\gamma = \zeta_2 - \zeta_1$ appearing in Eq. (18) and representing the relative spin azimuthal angle will be randomized.

Integrating over all orientations (and properly normalizing by 8π) we find therefore a lower bound for the mass ratio dependent final spin as:

$$\chi_f^{prec}(\chi_i, q) = \frac{1}{8\pi} \int_0^{2\pi} \int_{-1}^1 \int_{-1}^1 \chi_f(\chi_i, q, \kappa_i, \gamma) d\cos\kappa_1 d\cos\kappa_2 d\gamma. \quad (19)$$

The final spin χ_f^{prec} for precessing mergers (random configurations) as function of $\chi_1 = \chi_2$ and $\log q$ is

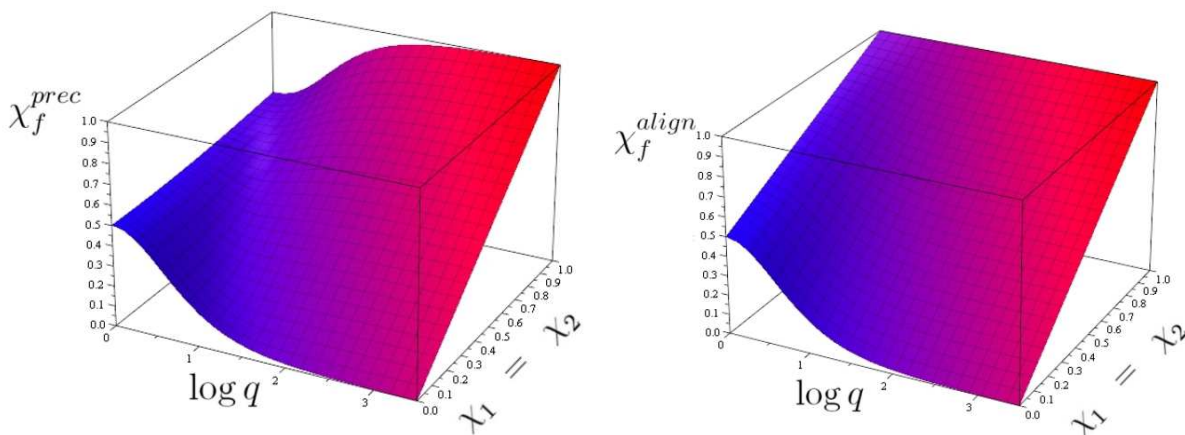


FIG. 3: (Color online) The typical final spin in supermassive black hole mergers as function of $\chi_1 = \chi_2$ and $\log q$, represented for precessing mergers (averaged over random configurations) - left panel; and mergers with the spins and orbital angular momentum fully aligned - right panel.

2. Typical final spin in precessing mergers

We establish an overall typical final spin for precessing mergers by integrating Eq. (19) over all possible mass ratios, weighted with the mass ratio dependent probability of encounters given in Eqs. (12):

$$\begin{aligned} \chi_f^{prec}(\chi_i) = & \int_1^{36} \chi_f^{prec}(\chi_i, q) \frac{dN(q)}{dq} \Big|_{q \in [1, 36]} dq \\ & + \int_{36}^{89} \chi_f^{prec}(\chi_i, q) \frac{dN(q)}{dq} \Big|_{q \in [36, 89]} dq \\ & + \int_{89}^{3000} \chi_f^{prec}(\chi_i, q) \frac{dN(q)}{dq} \Big|_{q \in [89, 3000]} dq \end{aligned} \quad (20)$$

The result of the numerical integration can be seen as the lower curve in Fig 4.

We note that for merging SMBHs in fast rotation $\chi_1 = \chi_2 \approx 0.998$ (the canonical spin limit, which occurs when

represented in the left panel of Fig. 3, as arising from a numerical integration (with approximation by the midpoint method). For equal masses the final spin ranges from 0.5 (for nonspinning black holes) to 0.6 (for maximally spinning black holes). This is consistent with the corresponding results of Ref. [20]. For $q \geq 100$ we have the test particle limit: the final spin is accurately approximated by χ_1 (in other words the orbital angular momentum does not modify the spin of the larger SMBH). In between there is the mass range with the most frequent encounters. For $q \approx 10$ for example the lower bound for the final spin ranges from 0.18 (nonspinning mergers) to 0.85 (maximally spinning mergers).

both the accretion and the radiation of the disk are taken into account [8]) the final spin becomes $\chi_f \approx 0.75$.

B. Non-precessing (aligned) mergers

There is no precession in the perfectly aligned configurations, when the two spins and the orbital angular momentum are parallel. Such configurations could arise due to accretion or by other mechanisms. We do not model such mechanisms here, just assume the alignment of the spins and orbital angular momenta of the two-body system.

1. The mass ratio dependent final spin

The spins being aligned to the orbital angular momentum implies $\kappa_i = 0 = \gamma$. Inserting these values in Eq.

(18), the final spin for non-precessing mergers as a function of the initial spin magnitudes and mass ratio takes a remarkably simple form:

$$\chi_f^{align}(\chi_i, q) = \frac{q^{-1}}{(1+q^{-1})^2} (2 + q\chi_1 + q^{-1}\chi_2) . \quad (21)$$

The final spin χ_f^{align} for non-precessing mergers is represented in the right panel of Fig 3 as function of $\chi_1 = \chi_2$ and $\log q$.

2. Typical final spin in non-precessing mergers

Next, we again integrate over the mass ratios, by properly weighting with the mass ratio dependent probability of encounters, as given in Eqs. (12):

$$\begin{aligned} \chi_f^{align}(\chi_i) &= \int_1^{36} \chi_f^{align}(\chi_i, q) \frac{d\mathcal{N}(q)}{dq} \Big|_{q \in [1,36]} dq \\ &+ \int_{36}^{89} \chi_f^{align}(\chi_i, q) \frac{d\mathcal{N}(q)}{dq} \Big|_{q \in [36,89]} dq \\ &+ \int_{89}^{3000} \chi_f^{align}(\chi_i, q) \frac{d\mathcal{N}(q)}{dq} \Big|_{q \in [89,3000]} dq \end{aligned} \quad (22)$$

The result of the numerical integration can be seen as the upper curve in Fig 4.

For merging SMBHs in fast rotation $\chi_1 = \chi_2 \approx 0.998$ (the canonical spin limit) the final spin is $\chi_f \approx 0.86$, much higher than for precessing mergers, however still reduced essentially as compared to the initial spin values.

V. CONCLUDING REMARKS

In this paper we have studied the typical mass ratio and the typical final spin in a two-body system composed of supermassive black holes (SMBH), thus we did not consider the perturbations induced by either of the accretion disks, nearby stellar population, magnetic fields or jets. SMBHs reside in the center of each galaxy and following the frequent galaxy mergers they also merge. Various dissipative processes, like dynamical friction, accretion and emitted gravitational radiation are responsible to their gradual approach and finally gravitational radiation is which drives them to coalescence through a sequence of inspiral, merger and ringdown.

By starting from precise and new data on the SMBH mass distribution we derived both a differential and an integral mass function, shown on Fig. 1. The differential mass function is a broken power law, with coefficients -1 and -3 , with the breakpoint at $8.9 \times 10^7 M_\odot$.

Then, exploiting a number of simple and reasonable assumptions we derived the mass ratio dependent probability of encounters of two such SMBHs, represented on Fig. 2. This confirms our expectation that the most frequent (approximately half of the) encounters are for

mass ratios $1 : 3$ to $1 : 30$, the interesting mass ratio range where a spin-flip would occur during the inspiral [16].

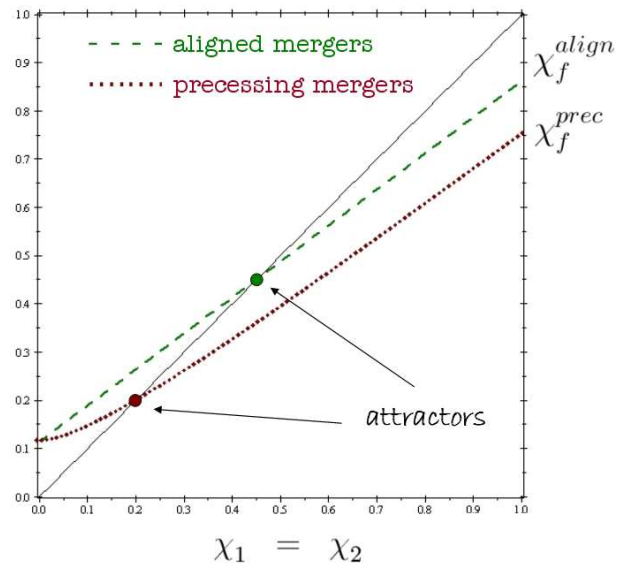


FIG. 4: (Color online) The typical final spin χ_f as function of $\chi_1 = \chi_2$ only, in the randomly precessing and the non-precessing merger limits (lower and upper curves, respectively). The curves are obtained by integration over all mass ratios of the expressions (19) $\chi_f^{prec}(\chi_1 = \chi_2, q)$ and (21) $\chi_f^{align}(\chi_1 = \chi_2, q)$, respectively, weighted with the mass ratio dependent probabilities of encounter (12). The line of equal initial and final spins is also indicated. Where this line crosses the final spin curves, there are two attractors (denoted by large dots), to where the final spin would converge after a sequence of mergers in the two scenarios.

Next, based on certain well-founded assumptions we derived a simple analytical expression for the final spin of such a merger, depending on the mass ratio, initial spin magnitudes, and orientation of the spins with respect to the orbital plane and each other. This formula approximates well more cumbersome expressions obtained from the fit with numerical simulations, and it is much simpler, thus advantageous in order to carry on the cumbersome numerical integrations which followed.

We proceeded to find the typical final spin in two limiting and highly idealized scenarios. First we allowed for perfectly random orientations (precessing case), over which we have integrated, obtaining a final spin still depending on the initial spin magnitudes and mass ratio. Then we folded with the derived mass ratio dependent merger rate, we integrated over the mass ratio, deriving a lower bound to the typical final spin value after mergers.

Secondly we considered the non-precessing configuration, with all spins and the orbital angular momentum perfectly aligned. Folding the final spin for this particular configuration again with the derived mass ratio dependent merger rate and integrating over the mass ratio

we obtained an upper bound for the typical spin. These are represented as function of the initial spin magnitudes (chosen to be equal³) on Fig. 4. A third curve, the line of equal initial and final spins is also indicated on the figure. The fact that both slopes of χ_f as function of the initial spins are smaller than one, leads to important consequences.

If we imagine a sequence of idealized (either randomly precessing or non-precessing) mergers, what happens is that low spins tend to increase by mergers while high spins decrease. There are in fact two attractors at $\chi_f^{prec} = 0.2$ and $\chi_f^{align} = 0.45$, respectively, where the spins converge after a reasonable number of the two types of mergers.

Real mergers, biased toward partial alignment by interactions with the environment (accretion, host galaxy, etc.) would generate a typical final spin lying between these two limiting values. Indeed, for example the galaxy group distribution around NGC383⁴ looks like a spindle, with the spin of the central black hole in the dominant galaxy, NGC383, aligned with the long axis of the spindle. This shows a correlation between the dominant galaxy black hole spin and the distribution of the other galaxies, all with central black holes as well. It is to be expected that the distribution of galaxies in the environment of a dominant galaxy is not random, but correlated, such that in a merger of a galaxy with the dominant galaxy the final spin, depending on the nature of the correlation, could fall anywhere between the two curves shown of Fig. 4.

After the merger episode gaseous accretion can start to increase the spin again. If gaseous accretion were strong, then the spin could become quite large in relatively short time. We propose to work out quantitatively such a model in a forthcoming work.

VI. ACKNOWLEDGEMENTS

This work has been realized in large part during two visits of LAG at the Institute of Radioastronomy Bonn, supported through STSM grants of the COST Action MP0905 "Black Holes in a Violent Universe".

Appendix A: Comparison of the final spin formula with related results

Various papers have presented empirical formulae for the final spin, with the functional form partially motivated by PN expressions and coefficients fitted to the

³ The second dimensionless spin parameter χ_2 will anyhow have but a small impact on the result, as the ratio of the *total* spins S_i scales with the mass ratio squared.

⁴ This is also known as the 3C31 radio source, cf. the NASA Extragalactic Database.

result of numerical runs. In one of the latest such works Barausse and Rezzola [39] suggested a set of criteria I-V) such a formula should obey. We compare this formula with our Eq. (18).

The condition I) of Ref. [39] implies no rest mass loss by gravitational radiation; our lower spin limit estimate with $\epsilon_{GW} = 0$ does the same. Condition III) assumes that the radiation loss in the last stage of the merger is along the direction of the total angular momentum, this property continuing to hold similarly as during the inspiral [33]. By identifying χ_f with \mathfrak{J} we also assume that. Similarly, this identification assures the validity of condition IV), which translates to no change in κ_i and γ during the plunge. However we note that in the strict sense the spin-spin and quadrupole-monopole couplings of the PN dynamics will obstruct this assumption; therefore this assumption cannot be considered valid for any distance, as assumed in Ref. [39]. Nevertheless these angular evolutions are negligible on the orbital timescale, thus during the plunge (over which we assume its validity and which lasts only from a fraction of an orbit to a few orbits) the condition can be regarded as accurate. Condition V. of Ref. [39] implies that the initial spins should drop out completely from the final spin formula in the particular case of equal masses and equal, but opposed spins. Our Eq. (16) can be specified for this configuration by inserting $\nu = 1$, $\chi_2 = \chi_1$, $\cos \gamma = -1$ and $\cos \kappa_2 = -\cos \kappa_1$ and it gives $\chi_f^{spec.config.} = \epsilon_f^{-1/2}/4$, which is also independent of the initial spins. Therefore condition V) also holds.

Finally, condition II) assumes that there are three vectors with conserved length. These are the two spins (that we also assume), and the vector $\mathbf{L}_N - \mathbf{J} + \mathbf{S}_f$ (what we do not). The latter condition in our notation implies

$$\begin{aligned} \text{const.} &= \left(\epsilon^{-1/2} \hat{\mathbf{L}}_N - (\mathfrak{J} - \eta^{-1} \chi_f) \hat{\mathbf{J}} \right)^2 \\ &= \epsilon^{-1} + (\mathfrak{J} - \eta^{-1} \chi_f)^2 \\ &\quad - 2\epsilon^{-1/2} (\mathfrak{J} - \eta^{-1} \chi_f) \hat{\mathbf{L}}_N \cdot \hat{\mathbf{J}}. \end{aligned} \quad (\text{A1})$$

We can set the constant to ϵ_f^{-1} by evaluating the formula at ϵ_f , where $\chi_f = \eta \mathfrak{J}_f$. Note that $\epsilon^{-1} \propto r$ thus it changes with \dot{r} , at Keplerian order. For generic r we have $\chi_f = \text{const.}$ and \mathfrak{J} changing significantly only on the radiation timescale (due to gravitational radiation). Over the orbital timescale the change in \mathfrak{J} by gravitational radiation backreaction is at 2.5PN orders, while over the precessional timescale is of 1PN order. The evolution of $\alpha = \cos^{-1}(\hat{\mathbf{L}}_N \cdot \hat{\mathbf{J}})$ generates a 1PN change over the orbital timescale [41], therefore the leading order changes over the orbital timescale of the second and third terms in the second line on the right hand side of Eq. (A1) are of order $\epsilon^{5/2}$ and $\epsilon^{1/2}$. Thus we conclude that condition II) concerning the constancy of the length of the vector $\mathbf{L}_N - \mathbf{J} + \mathbf{S}_f$ cannot be extended to arbitrary r , as in fact changes with $\epsilon^{1/2}$.

In the most generic case discussed in Ref. [39], their

Eqs. (6) and (8) reproduce our Eq. (16), provided we replace their $|\ell|$, given by their Eq. (10) and rewritten in our notations as

$$|\ell| = 2\sqrt{3} - 3.5171 \frac{\nu}{(1+\nu)^2} + 2.5763 \frac{\nu^2}{(1+\nu)^4} + \frac{0.4537 \frac{\nu}{(1+\nu)^2} - 0.8904}{1+\nu^2} (\chi_1 \cos \kappa_1 + \nu^2 \chi_2 \cos \kappa_2) - \frac{0.1229}{(1+\nu^2)^2} (\chi_1^2 + \nu^4 \chi_2^2 + 2\nu^2 \chi_1 \chi_2 \cos \gamma) \quad (\text{A2})$$

with $\varepsilon_f^{-1/2}$. In what follows, we compare the two values

(16) for the final spin, once computed by replacing $\varepsilon_f^{-1/2}$ with $|\ell|$ given by Eq. (A2), then with $\varepsilon_f^{-1/2} = 2$. For example in the equal mass $\nu = 1$, equal spin $\chi_1 = \chi_2$ case, when the spins are opposed to each other, thus $\gamma = \pi$ and $\kappa_2 = \pi - \kappa_1$, the ratio χ_f^{BR}/χ_f is identically 1.37, regardless of the values of $\chi_1 = \chi_2$ and κ_1 , therefore χ_f underestimates χ_f^{BR} . Various other configurations, all for equal dimensionless spins $\chi_2 = \chi_1$, are represented on Figs. 5 and 6.

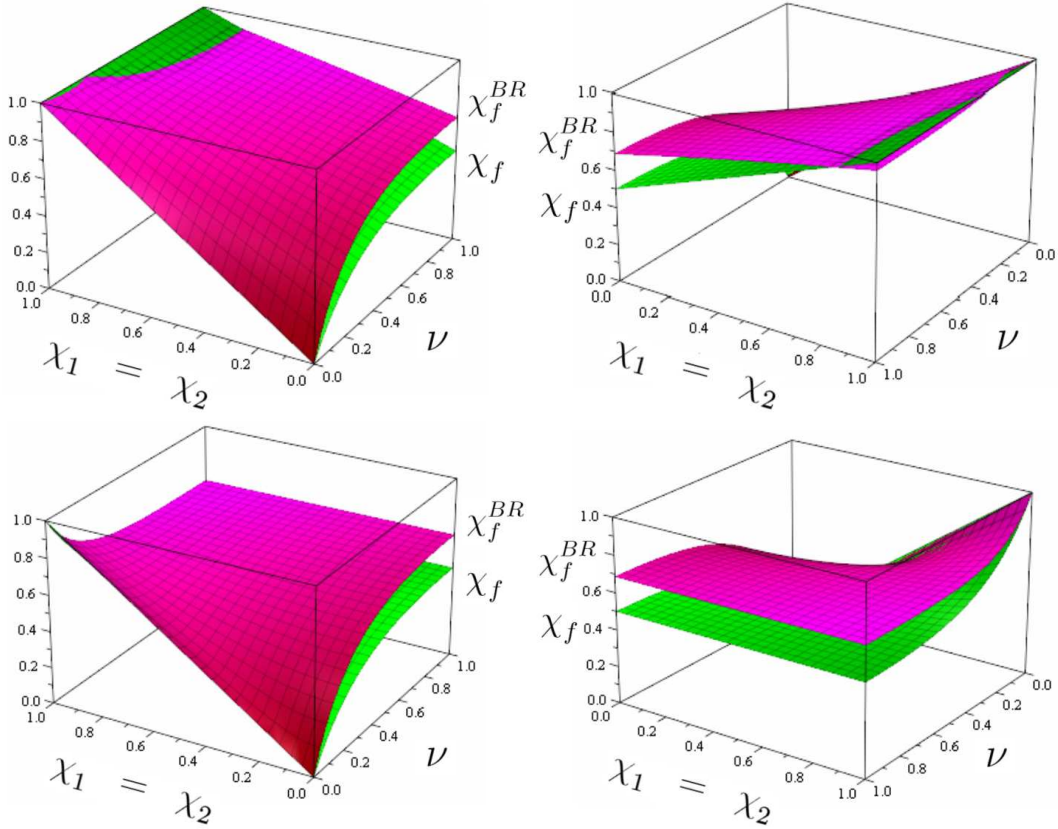


FIG. 5: (Color online) The final spin estimates χ_f (green surfaces) and χ_f^{BR} (magenta) as function of $\chi_1 = \chi_2$ and ν for perfect alignment of the spins with the orbital angular momentum (non-precessing case - upper row); and anti-aligned spins in the plane of motion (severe precession - lower row). Except a narrow parameter range with high mass ratio and high spin values in the upper row configuration, the estimated χ_f is smaller than χ_f^{BR} . The agreement increases with decreasing ν ; for the aligned configuration (upper row) is better in the high spin regime (visible on the right panel), then for low spin (left).

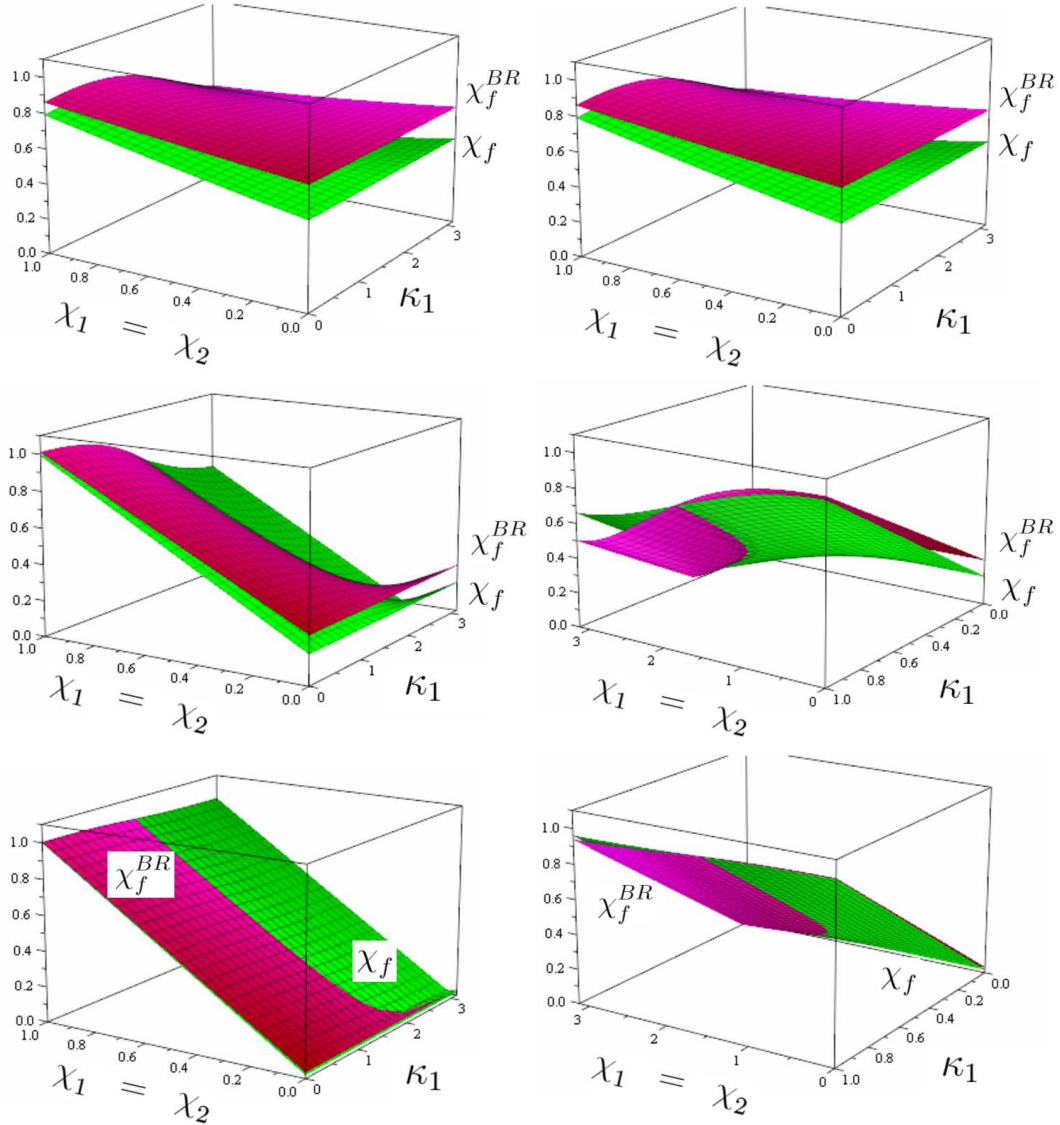


FIG. 6: (Color online) The final spin estimates χ_f (green surfaces) and χ_f^{BR} (magenta) as function of $\chi_1 = \chi_2$ and κ_1 for mass ratios $\nu = 1$ (upper row), $\nu = 0.1$ (middle row) and $\nu = 0.01$ (lower row). The represented configuration has the smaller spin confined to the plane of motion and the larger spin lying in the plane span by the smaller spin and orbital angular momentum. The agreement increases with decreasing ν (with $\chi_f < \chi_f^{BR}$ at large ν); is better in the high spin regime (visible on the right panel), then for low spin (left); is also better for configurations with $\kappa_1 \in [0, \pi/2]$ than for the severely misaligned configurations.

[1] B. Abbott et al. (LIGO Scientific Collaboration), *Rept. Prog. Phys.* **72**, 076901 (2009).
 [2] F. Acernese et al., *Class. Quantum Grav.* **25**, 184001 (2008).
 [3] H. Grote and the LIGO Scientific Collaboration, *Class. Quantum Grav.* **25**, 114043 (2008).
 [4] J. R. Gair, I. Mandel, M. C. Miller, M. Volonteri, *Gen. Relativ. Gravit.* **43** 485 (2011).
 [5] S. A. Farrell, N. A. Webb, D. Barret, O. Godet, J. M. Rodrigues, *Nature* **460**, 73 (2009); M. Mezcua, A. P. Lobanov, *Compact radio emission in Ultra Luminous X-ray sources*, E-print: arXiv:1011.0946, Proceedings of

the conference "Ultra-Luminous X-ray sources and Middle Weight Black Holes", to appear in *Astronomische Nachrichten*.
 [6] J. Kormendy, N. Drory, R. Bender, M. E. Cornell, *Astrophys. J.* **723**, 54 (2010).
 [7] J. M. Bardeen, *Nature* **226**, 64 (1970).
 [8] D. N. Page, K. S. Thorne, *Astrophys. J.* **191**, 499 (1974)
 [9] M. Abramowicz, M. Jaroszynski, M. Sikora, *Astron. Astrophys.*, **63**, 221 (1978); R. D. Blandford, R. L. Znajek, *Month. Not. Roy. Astr. Soc.* **179**, 433 (1977); M. Camenzind, *Astron. & Astroph.* **156**, 137 (1986); M. Camenzind, *Astron. & Astroph.* **162**, 32 (1986); M. Camen-

- zind, *Astron. & Astroph.* **184**, 341 (1987); M. Takahashi, S. Nitta, Y. Tamematsu, A. Tomimatsu, *Astrophys. J.* **363**, 206 (1990); S. Y. Nitta, M. Takahashi, A. Tomimatsu, *Phys. Rev. D* **44**, 2295 (1991); K. Hirovani, M. Takahashi, S. Nitta, A. Tomimatsu, *Astrophys. J.* **386**, 455 (1992); H. Falcke, P. L. Biermann, *Astron. & Astroph.* **293**, 665 (1995); L. X. Li, *Astrophys. J.* **533**, L115 (2000); D. X. Wang, K. Xiao, W. H. Lei, *Month. Not. Roy. Astr. Soc.* **335**, 655 (2002); D. A. Uzdensky, *Astrophys. J.* **620**, 889 (2005); Z. Kovács, P. L. Biermann, L. Á. Gergely, *Mon. Not. Royal Astron. Soc.* **416**, 991 (2011); Z. Kovács, L. Á. Gergely, M. Vasúth, *Phys. Rev. D* **84**, 024018 (2011).
- [10] J. P. Leahy, T. W. B. Muxlow, P. W. Stephens, *Monthly Not. Royal Astron. Soc.* **239**, 401 (1989); C. L. Carilli, R. A. Perley, J. W. Dreher, J. P. Leahy, *Astrophys. J.* **383**, 554 (1991); A. Celotti, A. C. Fabian, *Monthly Not. Royal Astron. Soc.* **264**, 228 (1993); W. J. Duschl, H. Lesch, *Astron. Astrophys.* **286**, 431 (1994).
- [11] P. L. Biermann, J. K. Becker, L. Caramete, L. Á. Gergely, I. C. Mariş, A. Meli, V. de Souza, T. Stanev, *Int. J. Mod. Phys. D* **18** 1577 (2009); P. L. Biermann, J. K. Becker, L. Caramete, A. Curutiu, R. Engel, H. Falcke, L. Á. Gergely, P. G. Isar, I. C. Mariş, A. Meli, K.-H. Kampert, T. Stanev, O. Taşcau, C. Zier, *Nucl. Phys. B, Proc. Suppl.* **190**, 61 (2009); Gopal-Krishna, P. L. Biermann, V. de Souza, P. J. Wiita, *Astrophys. J. Lett.* **720**, L155 (2010); P. L. Biermann, V. de Souza, *Astrophys. J.* **746**, 72 (2012).
- [12] Ch. Zier, *Monthly Not. Royal Astron. Soc. Lett.* **371**, L36 (2006).
- [13] T. Alexander, in *2007 STScl Spring Symp.: Black Holes*, ed. M. Livio & A. M. Koekemoer (Cambridge: Cambridge Univ. Press), E-print: arXiv:0708.0688.
- [14] A. Sesana, F. Haardt, P. Madau, *Astrophys. J.* **651**, 392 (2006); A. Sesana, F. Haardt, P. Madau, *Astrophys. J.* **660**, 546 (2007); A. Sesana, F. Haardt, P. Madau, *Astrophys. J.* in press (2007), arXiv:0710.4301.
- [15] K. Hayasaki, *PASJ* (2008), E-print: arXiv:0805.3408.
- [16] L. Á. Gergely, P. L. Biermann, *Astrophys. J.* **697**, 1621 (2009).
- [17] K. G. Arun, S. Babak, E. Berti, N. Cornish, C. Cutler, J. Gair, S. A. Hughes, B. R. Iyer, R. N. Lang, I. Mandel, E. K. Porter, B. S. Sathyaprakash, S. Sinha, A. M. Sintes, M. Trias, C. Van Den Broeck, M. Volonteri, *Class. Quantum Grav.* **26**, 094027 (2009); R. N. Lang, S. A. Hughes, *Class. Quantum Grav.* **26**, 094035 (2009).
- [18] J. M. Bardeen, J. A. Petterson, *Astrophys. J.* **195**, L65 (1975).
- [19] S. A. Hughes, R. D. Blandford, *Astrophys. J.* **585**, L101 (2003).
- [20] E. Berti, M. Volonteri, *Astrophys. J.* **684**, 822 (2008).
- [21] L. Á. Gergely, P. L. Biermann, L. I. Caramete, *Class. Quantum Grav.* **27**, 194009 (2010).
- [22] L. I. Caramete, P. L. Biermann, *Astron. Astroph.* **521**, A55 (2010).
- [23] W. H. Press, P. Schechter, *Astrophys. J.* **187**, 425 (1974).
- [24] A. S. Wilson, E. J. M. Colbert, *Astrophys. J.* **438**, 62 (1995).
- [25] T. R. Lauer et al., *Astrophys. J.* **662**, 808L (2007).
- [26] L. Ferrarese et al., *Astrophys. J. Suppl. Ser.* **164**, 334 (2006).
- [27] P. Côté, S. Piatek, L. Ferrarese, et al., *Astrophys. J. Suppl. Ser.* **165**, 57 (2006).
- [28] J. Magorrian et al., *Astronomical J.* **115**, 2285 (1998).
- [29] A. J. Benson, D. Džanović, C. S. Frenk, R. Sharples, *Mon. Not. Roy. Astron. Soc.* **379**, 841 (2007).
- [30] G. Gilmore et al., *Nucl. Phys. B* **173**, 15 (2007).
- [31] A. Klypin, H.-S. Zhao, R. S. Somerville, *Astrophys. J.* **573**, 597 (2002).
- [32] B. M. Barker, R. F. O'Connell, *Phys. Rev. D* **12**, 329 (1975); B. M. Barker, R. F. O'Connell, *Gen. Relativ. Gravit.* **11**, 149 (1979).
- [33] A. Apostolatos, C. Cutler, G. J. Sussman, K. S. Thorne, *Phys. Rev. D* **49**, 6274 (1994).
- [34] L. Á. Gergely, Z. I. Perjés, M. Vasúth, *Phys. Rev. D* **58**, 124001 (1998).
- [35] L. Á. Gergely, *Phys. Rev. D* **61**, 024035 (1999).
- [36] L. Á. Gergely, Z. Keresztes, *Phys. Rev. D* **67**, 024020 (2003).
- [37] L. Á. Gergely, *Phys. Rev. D* **62**, 024007 (2000).
- [38] L. Rezzolla, E. Barausse, E. Nils Dorband, D. Pollney, C. Reisswig, J. Seiler, S. Husa, *Phys. Rev. D* **78** 044002 (2008); M. C. Washik, J. Healy, F. Herrmann, I. Hinder, D. M. Shoemaker, P. Laguna, R. A. Matzner, *Phys. Rev. Lett.* **101** 061102 (2008); A. Buonanno, L. E. Kidder, L. Lehner, *Phys. Rev. D* **77** 026004 (2008); W. Tichy, P. Marronetti, *Phys. Rev. D* **78**, 081501(R) (2008); U. Sperhake, V. Cardoso, F. Pretorius, E. Berti, T. Hinderer, N. Yunes, *Phys. Rev. Lett.* **103**, 131102 (2009); J. Healy, P. Laguna, R. A. Matzner, D. M. Shoemaker, *Phys. Rev. D* **81**, 081501 (2010); E. Barausse, *The importance of precession in modelling the direction of the final spin from a black-hole merger*, E-print: arXiv:0911.1274 (2009); M. Kesden, U. Sperhake, E. Berti, *Phys. Rev. D* **81**, 084054 (2010); C. O. Lousto, M. Campanelli, Y. Zlochower, H. Nakano, *Class. Quantum Grav.* **27**, 114006 (2010).
- [39] E. Barausse, L. Rezzolla, *Astrophys. J. Lett.* **704** L40-L44 (2009).
- [40] J. E. Greene, A. J. Barth, L. C. Ho, *New Astron. Rev.* **50**, 739 (2006); J. E. Greene, L. C. Ho, *Astrophys. J.* **641**, L21 (2006).
- [41] L. Á. Gergely, *Phys. Rev. D* **81**, 084025 (2010); L. Á. Gergely, *Phys. Rev. D* **82**, 104031 (2010).